Interaction of 4-Arylcoumarin Analogues of Combretastatins with Microtubule Network of HBL100 Cells and Binding to Tubulin †

ARTICLE *in* BIOCHEMISTRY · SEPTEMBER 2006

Impact Factor: 3.02 · DOI: 10.1021/bi060476g · Source: PubMed

Interaction of 4-Arylcoumarin Analogues of Combretastatins with Microtubule Network of HBL100 Cells and Binding to Tubulin†

Catherine Rappl,‡ Pascale Barbier,*,‡ Véronique Bourgarel-Rey,‡ Catherine Grégoire,‖ Robert Gilli,‡ Manon Carre,‡ Sébastien Combes,§ Jean-Pierre Finet,§ and Vincent Peyrot‡

FRE-CNRS 2737, Universités Aix-Marseille 1 et 2, ≪ Cytosquelette et Intégration des Signaux du Micro-Environnement Tumoral ≫, 27 boulevard Jean Moulin, 13385 Marseille Cedex 5, France, UMR-CNRS 6517, Universités Aix-Marseille 1, 2 et 3, ≪ Chimie, Biologie et Radicaux Libres ≫, Faculté des Sciences de St-Jérôme, case 521, 13397 Marseille Cedex 20, France, and INSERM U710, Université de Montpellier II-EPHE, place Eugène Bataillon, cc105, Bat 24, 3ème étage extension, 34095 Montpellier Cedex 5, France

Received March 10, 2006; Revised Manuscript Received June 7, 2006

ABSTRACT: The synthesis of different 4-arylcoumarin analogues of combretastatin A-4 led to the identification of two new compounds (**1** and **2**) with potent cytotoxic activity on a CEM leukemia cell line and a third one completely inactive (compound **3**). It was suggested that the cytotoxicity of compounds **1** and **2** may be related to their interaction with microtubules and tubulin, since these compounds inhibit microtubule formation from purified tubulin in vitro [Bailly et al. (2003) *J. Med. Chem*. *46* (25), 5437−5444]. In the present study, tubulin was identified as the main target of these molecules. We studied structure−activity relationships of these compounds using biological experiments specific for tubulin binding. The modification of cell cycle progression induced by compounds **1** and **2** was characterized by an apoptotic induction on human breast cells (HBL100). In addition, these two molecules disturbed cell survival by depolymerizing the microtubule network, leading to a mitotic block. We then determined the thermodynamic parameters of their interaction with purified tubulin by fluorescence spectroscopy and isothermal microcalorimetry. These results, together with a superimposition of the molecule on colchicine in the X-ray-determined three-dimensional structure model of tubulin−colchicine complex, allowed us to identify the pharmacophore of the combretastatin A-4 analogues responsible for their biological activity.

The microtubule network is an essential component of the cytoskeleton in eukaryotic cells. The cytostatic drug colchicine was shown to bind tubulin, the main constitutive protein of microtubules. This fundamental step in the development of new antimitotic agents then led to new cancer chemotherapy approaches and to a better knowledge of microtubule pharmacology and biochemistry. Antimitotic drugs that bind tubulin, also called antitubulin agents, are classified as microtubule-stabilizing agents or microtubule-destabilizing agents. Taxoids (paclitaxel and docetaxel) enhance the tubulin polymerization and interact directly with microtubules, stabilizing them against depolymerization. The *Vinca* alkaloids and the colchicinoids inhibit tubulin polymerization but differ in their mechanism of action and in their binding site on tubulin (*1*). Until now, only molecules from *Vinca* alkaloids and taxoid groups were extensively used in cancer chemotherapies. Considering the success of the antitubulin pharmacological class, numerous researches are now focused on the discovery and clinical trial development of new derivatives. Combretastatin A-4, already known as a powerful inhibitor of tubulin polymerization and cell growth (*2*), also has an antivascular activity at low concentration (*3*). This new low-concentration activity of combretastatin A-4 led to the renewal of interest for the possible clinical use of colchicine analogues often discarded for their large neurotoxicity. Moreover, tumor cells can acquire resistance properties to various anticancer agents. Overexpression of the drug efflux transporter P-glycoprotein causes this multidrug-resistance phenotype and contributes to the failure of cancer chemotherapy. The combretastatin A-4 is not recognized by this glycoprotein. Because of this latter characteristic and of its antiangiogenic property, combretastatin A-4 became the most interesting antitubulin agent which interacts with the colchicine binding site. However, natural combretastatin A-4 suffers from serious drawbacks: it isomerizes to an inactive form (*4*) and has a low aqueous solubility. Therefore, efforts have focused on making soluble combretastatin A-4 derivatives and blocking isomerization (*5*). A set of 4-arylcoumarin analogues of combretastatin A-4 have thus been synthesized, and their cytotoxicity on human leukemia CEM cell line have been assessed (*6*). Among this set of molecules, compounds **1**[1] and **2** (Scheme 1) significantly decreased CEM cell growth and inhibited purified tubulin polymerization. They can therefore be considered as functional analogues of combretastatin A-4 (*6*).

The aim of this study was to establish a structure−activity relationship of compounds **1** and **2** in the context of their binding to tubulin and to compare it to combretastatin A-4

† This work was supported in part by INTAS (Grant No. 03-514-915).

* Corresponding author. E-mail, Pascale.barbier@pharmacie.univ-mrs.fr; tel., 33-4-91-83-56-16; fax, 33-4-91-83-55-05.

‡ FRE-CNRS 2737, Universités Aix-Marseille.

§ UMR-CNRS 6517, Universités Aix-Marseille.

‖ INSERM U710, Université de Montpellier II-EPHE.

10.1021/bi060476g CCC: $33.50
Published on Web 07/07/2006

Scheme 1: Structure of Colchicine, Combretastatin A-4, and the 4-Arylcoumarin Analogues **1**, **2**, and **3**

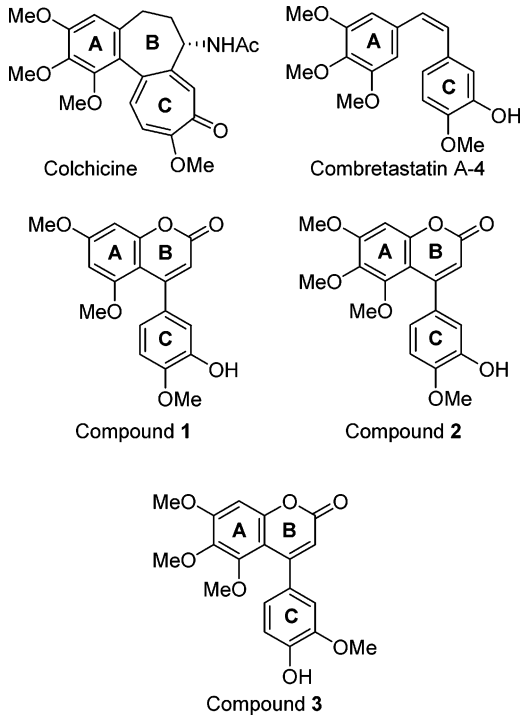

and an inactive compound of the series (compound **3**). We have studied the activity of these molecules on the cellular microtubule network by immunofluorescence and on the cell cycle of human breast cell line. We have also characterized the thermodynamic parameters of these compounds' interaction with tubulin by isothermal titration microcalorimetry and intrinsic tryptophan fluorescence. By molecular modeling, we have superimposed all the molecules on the colchicine in the colchicine binding site using the recently determined X-ray three-dimensional structure of the tubulin−colchicine complex (*7*), and we have identified the structural part of the compound **1** responsible for its biological activity.

MATERIALS AND METHODS

Drugs. The synthesis of the 4-arylcoumarin analogues of combretastatin A-4 was done as previously described by Bailly et al. (*6*), and their structures are represented in Scheme 1. The concentrations of compound **1**, compound **2**, and compound **3** were measured spectrophotometrically with a Perkin-Elmer Lambda 800 spectrophotometer at 324 nm with extinction coefficients of 15124, 13618, and 13917 M^{-1} cm^{-1}. Combretastatin A-4 (Scheme 1) was obtained from Tocris Bioscience (Avonmouth, U.K.). Its concentration was measured spectrophotometrically at 290 nm using an extinction coefficient of 9161 M^{-1} cm^{-1}.

Cell Culture. Human epithelial mammary HBL100 cells were grown in Dubelcco's modified Eagle medium (DMEM, Gibco) supplemented with 10% fetal bovine serum (FBS), 2 mM L-glutamine, and 1% penicillin/streptomycin (Gibco) and maintained in a humidified incubator at 37 °C with 5% CO_2. For experiments, exponentially growing cells (2.6×10^4 cells/cm^2) were seeded 24 h before drug treatment.

Cytotoxicity Tests. Cells were seeded in 96-well plates to be treated during 72 h. The numbers of viable cells were estimated by using the colorimetric 3-(4,5-dimethylthiazol-2-yl)-2,5-diphenyltetrazolium bromide (MTT; Sigma) assay, and absorbance was measured at 550 nm with a Dynatech MR 7-000 plate reader. Three independent experiments were performed, and the IC_{50} values (i.e., concentration half-inhibiting cell proliferation) were graphically determined.

Flow Cytometry Analysis. Cells were cultured in 6-well plates. After 18 or 48 h of treatment, cells were trypsinized and fixed in cold methanol (70%, 20 min at −20 °C), washed, and resuspended in phosphate-buffered saline solution (PBS). The cells were then stained with propidium iodide (20μg/mL) for 10 min at room temperature. DNA content was measured by flow cytometry (Becton Dickinson FAC Sort), and the percentages of cells in different cell-cycle phases were determined.

Fluorescence Microscopy. For immunofluorescence microscopy of the microtubule network, cells were plated on 8-well chamber slides (Labtek) and incubated with the different drugs during 5 h. Cells were then fixed in 3.7% formaldehyde for 10 min, permeabilized with PBS-saponine 0.1% for 30 min, and stained with an α-tubulin antibody (1:400 in PBS−BSA 1%; Sigma) and an FITC-conjugated secondary antibody (1:20, Jackson Immunoresearch). For nuclei visualization, cells were treated with combretastatin analogues for 18 h (doubling time) and fixed before incubation for 10 min with 0.25 μg/mL 4′,6-diamidino-2-phenylindole (DAPI; Sigma Aldrich) in the dark. All cells were observed using a Leica DM-IRBE microscope coupled with a digital camera (CoolsnapFX; Princeton Instruments) and analyzed with Metamorph software. About 500 DAPI-stained cells were examined to quantify the percentages of cells in interphase, mitosis, and apoptosis.

Tubulin Purification. Tubulin was extracted from lamb brains by ammonium sulfate fractionation and ion exchange chromatography and stored in liquid nitrogen (*8*, *9*, *10*). Before use, aliquots of protein were chromatographed in drained spin columns (1 × 5 cm) of Sephadex G25, equilibrated with PG buffer (20 mM sodium phosphate, 0.1 mM GTP, pH 7), followed by passage through a gravity column of Sephadex G25 (1 × 10 cm) and equilibrated with the same buffer. Protein concentration was measured spectrophotometrically with a Perkin-Elmer spectrophotometer Lambda 800 at 275 nm with an extinction coefficient of 1.09 L g^{-1} cm^{-1} in guanidine hydrochloride or 1.07 L g^{-1} cm^{-1} in 0.5% SDS in neutral aqueous buffer.

Binding Measurement by Fluorescence Titration. Fluorescence measurements were performed with a Perkin-Elmer luminescence spectrometer 50 with slit widths of 10/10 nm. Uncorrected fluorescence spectra were obtained in PG buffer, pH 7, by using 0.2 (excitation direction) × 1 cm cells (Hellma) thermostated at 25 °C by circulating water from

[1] Abbreviations: DAPI, 4′,6-diamidino-2-phenylindole; MTT, 3-(4,5-dimethylthiazol-2-yl)-2,5-diphenyltetrazolium bromide; DMEM, Dulbecco's modified Eagle's medium; FBS, fetal bovine serum; BSA, bovine serum albumin; PBS, phosphate-buffered saline solution; DNA, deoxyribonucleic acid; PG buffer, 20 mM sodium phosphate, 0.1 mM GTP, pH 7; SDS, sodium dodecyl sulfate; ITC, isothermal titration calorimetry; DMSO, dimethyl sulfoxide; DAMA-colchicine, *N*-deacetyl-*N*-(2-mercaptoacetyl)-colchicine; MTOC, microtubule organizing centers; ITC, isothermal titration calorimetry; PDB, Protein Data Base; compound **1**, 4-(3′-hydroxy-4′-methoxyphenyl)-5,7-dimethoxycoumarin; compound **2**, 4-(3′-hydroxy-4′-methoxyphenyl)-5,6,7-trimethoxycoumarin; compound **3**, 4-(4′-hydroxy-3′-methoxyphenyl)-5,6,7-trimethoxycoumarin.

an external water bath. Determination of the binding parameters was done by measuring quenching of the intrinsic protein fluorescence signal by ligands. Tubulin (1−4 μM) was titrated with various concentrations of combretastatin A-4 and analogues. Fluorescence measurements were performed with an excitation wavelength of 295 nm in order to specifically excite the tubulin tryptophanyl residues.

*1. Fluorescence Binding Titration for Compounds **1**−**3**.* Fluorescence emission was recorded at 340 nm. The inner filter effects were corrected according to Lakowicz (*11*) as follows:

$$F_{corr} = F_{obs} \exp\{(A_{exc} + A_{em})/2\}$$

F_{obs} and F_{corr} are the observed and corrected fluorescence values at the emission wavelengths. A_{exc} and A_{em} are the absorptions at the excitation and emission wavelengths, respectively, calculated with $A_x = \epsilon_x l_x C$, in which x is the excitation or emission direction, ϵ is the extinction coefficient, l is the path length of the cell in the excitation and emission directions, and C is the ligand concentration. The corrected quenching fluorescence titration curves were inverted and fitted to the saturation curve equation by means of nonlinear least-squares regression analysis.

$$F_{corr} = \frac{F_{max}[L_f]}{K_d + [L_f]}$$

F_{max} is the plateau fluorescence value. Concentrations (bound ligand $[L_b]$ and free ligand $[L_f]$) and binding parameters (the apparent stoichiometry n and the dissociation constant K_d) were determined with the following equation:

$$[L_b] = {}^1/2\{([L_0] + n[P_0] + K_d) - (([L_0] + n[P_0] + K_d)^2 - 4n[P_0][L_0])^{1/2}\}$$

where $[L_0]$ and $[P_0]$ are the total ligand and protein concentrations, respectively. The algorithm starts with an arbitrary opening set of n and K_d values. With these values, $[L_b]$ and $[L_f]$ are calculated, and then the nonlinear least-squares regression analyses are executed. The initial set is corrected in the next step by a Newton−Gauss procedure. This iterative procedure is continued until the minimum sum of squared deviations between experimental and calculated values of F_{corr} is obtained.

2. Fluorescence Binding Titration for Combretastatin A-4. In contrast to compounds **1**−**3**, combretastatin A-4 presents an intrinsic emission fluorescence signal from 350 to 550 nm with a maximum at 400 nm (λ_{exc} 295 nm) which overlays the intrinsic fluorescence emission spectra of tubulin. To determine the signal corresponding to the interaction, we calculated, for each concentration of the ligand, the fluorescence emission spectrum obtained if no binding occurred (S_{calc}), by a linear combination of the emission tubulin (S_{tub}), ligand alone spectra ($S_{A-4;i}$), and buffer S_{bu}. So, for each ligand concentration i, we may write

$$S_{calc;i} = A \times S_{tub} + B \times S_{A-4;i} + S_{bu}$$

A nonlinear regression, minimizing the sum of squared deviations with a Gauss−Newton method, was used to obtain the best fitting coefficients A and B (for an example, see the inset of Figure 4). The calculated spectra ($S_{calc;i}$) were then subtracted from the experimental emission spectra corresponding to the desired ligand concentration complex observed (S_{exp}). The intensities of the differential fluorescence ($\Delta F = S_{exp} - S_{cal}$) at a given wavelength (356 or 420 nm) were plotted versus the concentration of combretastatin A-4 and fitted as described for **1**, **2**, and **3**. All the fluorescence measurement experiments were done in PG buffer.

Binding Measurement by Isothermal Titration Calorimetry (ITC). Measurement of the binding of combretastatin A-4 to tubulin was carried out at 25 °C using a MicroCal MCS titration calorimeter. Enthalpy of binding (ΔH) and equilibrium constant (K_a) were obtained using the following procedure. Aliquots (5μL) of the ligand (0.36×10^{-3} M) were injected from a 250 μL microsyringe into the 1.34 mL calorimeter cell containing the tubulin solution ($(1.5-2.0) \times 10^{-5}$ M) to achieve a complete binding isotherm. The heat of dilution was measured by injecting the ligand into the buffer or by additional injections of ligand after saturation; the obtained value was subtracted from the heat of reaction to obtain the effective heat of binding. Titration curves were fitted using the MicroCal Origin software, assuming a single class of site. Binding measurements for compounds **1**−**3** were carried out at 25 °C by displacement ITC experiments (*12*, *13*) with combretastatin A-4 because of the absence of heat exchange in direct ITC analysis. Here, **1**−**3**, were displaced from the tubulin binding site by combretastatin A-4, the affinity of which had been directly measured by ITC ($K_a = 2.6 \times 10^7$ M^{-1}). Tubulin ($(1.5-5) \times 10^{-5}$ M) saturated with **1** (6×10^{-5} M), **2** (2×10^{-4} M), or **3** (4×10^{-4} M) was introduced into the calorimeter cell and titrated with 50 injections of 5−10 μL aliquots of the combretastatin A-4 (1×10^{-3} M). K_a values were obtained from the titration curve fit using the modified regression equations of Sigurskjold programmed for the Origin software (*13*). To avoid any problem of solubility of the compounds, all ITC experiments were done in PG buffer with 10% DMSO.

Analytical Ultracentrifugation. Sedimentation velocity experiments were performed with a Beckman Optima XLA analytical ultracentrifuge equipped with absorbance optics, using an An55Ti rotor and standard double-sector centerpieces. Identical samples of tubulin (2×10^{-6} M), without and with 50×10^{-6} M of ligand, were run simultaneously at 40 000 rpm at 20 °C in PG buffer. The apparent sedimentation coefficients were determined by fitting the velocity data using one noninteracting discrete species with the SEDFIT program (*14*).

Molecular Modeling. The Ampac 7.0 software was used to construct and optimize the combretastatin A-4, and the **1**−**3** analogues with the semiempirical AM1 method. The X-ray structure of the $\alpha\beta$-tubulin/*N*-deacetyl-*N*-(2-mercaptoacetyl)-colchicine (DAMA-colchicine) complex (*7*) (Protein Data Bank [PDB] 1SA0) was used in this study. After removal of the Stathmin-like domain and of the subunits C and D, the ligands were superimposed on the DAMA-colchicine in the tubulin site. Superimpositions of the (C22−C1−C3−C5−C7−C8) benzene trace (A- ring) of colchicine bound to tubulin, to the A-ring of combretastatin A-4, and compounds **1**−**3** were made using the Accelrys software InsightII and Builder modules (San Diego, CA), run on a Silicon Graphics O2 workstation (SGI, Mountain View, CA).

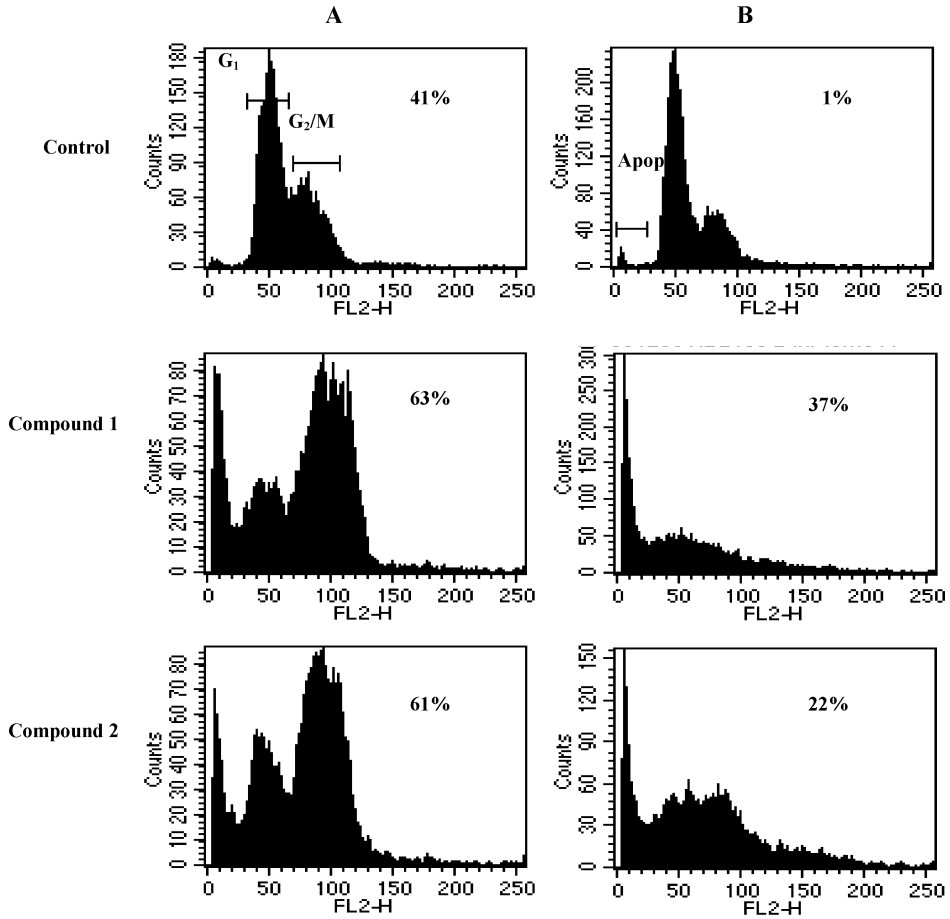

FIGURE 1: Effects of 4-arylcoumarin analogues (compounds **1** and **2**) on the cell cycle progression. HBL100 cells were treated for (A) 18 h and (B) 48 h with 1 μM of compounds **1** and **2**. Percentages of (A) G_2/M-arrested cells and (B) apoptotic (sub-G_0/G_1) cells are noted at 18 and 48 h, respectively.

RESULTS

Modification of Cell Cycle Progression and Induction of Apoptosis by the Combretastatin A-4 Analogues on HBL100 Cells. The cytotoxic activity of the different 4-arylcoumarin derivatives of combretastatin A-4 was assayed against human breast HBL100 cells (data not shown). Values of the half inhibitory proliferation concentrations (IC_{50}) were 87 $\pm$ 6 and 420 $\pm$ 10 nM for compounds **1** and **2,** respectively, while compound **3** was not cytotoxic. In this cell line, combretastatin A-4 was more cytotoxic than its analogues, as its IC_{50} was 2.0 $\pm$ 0.3 nM. By flow cytometry, we compared the modifications in the cell cycle progression induced by a same concentration (1 μM) of drug. Compounds **1** and **2** caused a massive accumulation of HBL100 cells in the G_2/M phase (more than 60%, Figure 1A), as observed with combretastatin A-4 (86%, data not shown). This G_2/M accumulation corresponded to a mitotic block, as determined by fluorescence microscopy (3% of control cells in mitosis, 44% and 32% with compounds **1** and **2**, respectively). This disturbance of cell cycle progression led to apoptosis induction, as shown by the enhanced accumulation of sub-G1 cells (Figure 1B) and visualization of fragmented nuclei by fluorescence microscopy (data not shown). In contrast, compound **3** did not lead to any change in the cell cycle phase distribution nor to apoptosis (40% in G_2/M and 1% in sub-G1 phase; data not shown). Thus, among the analogues of combretastatin A-4, compounds **1** and **2** modified the cell cycle progression and triggered cell death, whereas compound **3** was inactive.

Effect of Combretastatin A-4 and Analogues on HBL100 Microtubule Network. Since we have shown that combretastatin A-4 and compounds **1** and **2** inhibit the purified tubulin polymerization (*6*) (Table 1), we performed immunofluorescence staining of the microtubule network in HBL100 cells. The microtubule polymerization state was visualized after a 5 h-treatment with increasing drug concentrations (Figure 2). In the case of combretastatin A-4, microtubule depolymerization began at a concentration of 5 nM, was obvious at 10 nM, and total at 1 μM. When cells were treated with 1 μM of **1** or **2**, we observed a depolymerization of the microtubule network, which is total at 2 μM. At this concentration, only the microtubule organizing centers (MTOC) were still visible. Cell treatment with a lower concentration of drugs (500 nM) led to a partial depolymerization with compound **1** and showed a weaker effect with compound **2**. This concentration highlighted the difference in the depolymerizing activity between the two analogues and showed that **1** was the most efficient. Finally, no depolymerizing effect was observed for the analogue **3** in the range of concentrations tested (up to 10 μM). Thus, like combretastatin A-4, compounds **1** and **2** modified strongly the microtubule cytoskeleton organization in HBL100 cells.

Both analysis of DNA content and visualization of the microtubule network showed that analogue **1** is the most

Table 1: Inhibitory Effects on Microtubule Formation at 37 °C and Binding Parameters of Combretastatin A-4 and Analogues **1**, **2**, and **3** to Tubulin in PG Buffer, at 25 °C[a]

	half inhibitory molar ratio (ligand/tubulin) of microtubule formation in vitro[b]	K_a [M^{-1}][c]	K_a [M^{-1}]	ΔH [kJ mol^{-1}]	$T\Delta S$ [kJ mol^{-1}]
combretastatin A-4	0.07	$(3.35 \pm 1.46) \times 10^6$	$(1.88 \pm 0.23) \times 10^6$ [d]	-37.2 ± 3.3[d]	-1.7 ± 3.3[d]
compound **1**	0.28	$(3.75 \pm 1.23) \times 10^5$	$(1.11 \pm 0.20) \times 10^5$ [e]	nd[f]	28.9 ± 0.4[e]
compound **2**	1.45	$(6.72 \pm 0.88) \times 10^4$	$(1.66 \pm 0.61) \times 10^4$ [e]	nd[f]	24.3 ± 0.8[e]
compound **3**	inactive	$(4.01 \pm 1.05) \times 10^4$	$(2.79 \pm 2.60) \times 10^3$ [e]	nd[f]	19.7 ± 2.9[e]

[a] Values are the mean of three experiments. K_a and ΔH values are given $\pm$ the standard deviation (SD) of the mean. The errors on $T\Delta S$ values were calculated as $[SD^2_{(\Delta H)} + SD^2_{(\Delta G)}]^{1/2}$. [b] Determined by Bailly et al. (*6*). [c] K_a determined by fluorescence ligand titration. [d] K_a determined by isothermal titration microcalorimetry, direct method. [e] K_a determined by isothermal titration microcalorimetry, competition with combretastatin A-4. [f] nd, not determined.

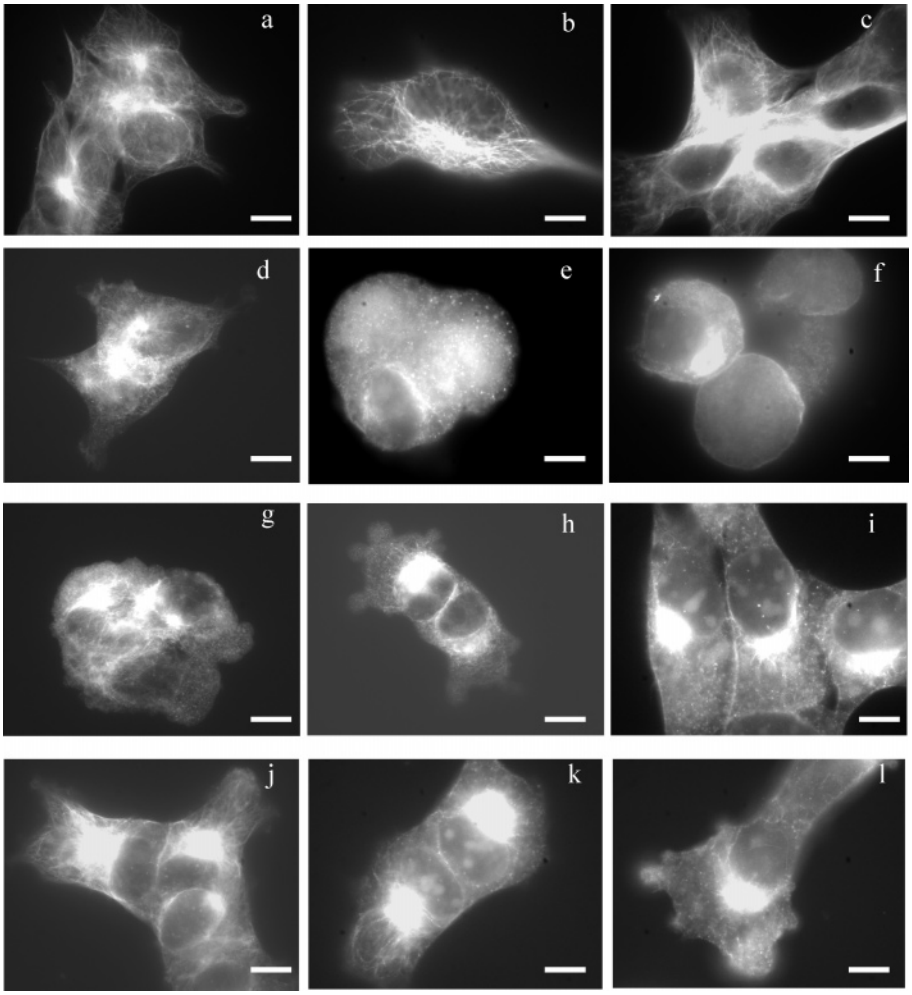

FIGURE 2: Indirect immunofluorescence staining of α-tubulin in HBL100 cells. (a) Control cells, (b, c) cells treated with 1 and 10 μM of compound **3,** respectively. Cells treated with 5 nM (d), 10 nM (e), and 1 μM (f) of combretastatin A-4. Cells treated with 500 nM (g), 1 μM (h), and 2 μM (i) of compound **1**. Cells treated with 500 nM (j), 1 μM (k), and 2 μM (l) of compound **2**. All observations were made after 5 h incubation with drugs. Scale bar = 5 μm.

active compound, but by comparison with combretastatin A-4, a 100-fold higher concentration is necessary to obtain a similar effect. Compound **2** shows an intermediate efficiency, and **3** is inactive in the range of concentrations used. To complete the structure−activity relationship, characterization of the thermodynamic parameters of the binding of combretastatin A-4 and of the three 4-arylcoumarin analogues to tubulin (compounds **1**−**3**) was performed.

Determination of the Thermodynamic Parameters of the Interaction of Combretastatin A-4 and Analogues with Tubulin. 1. Fluorescence Quenching of Tubulin. The uncorrected intrinsic fluorescence emission spectra of tubulin were examined by exciting the tryptophan residues at 295 nm. A decrease in emission intensity fluorescence at 340 nm was observed with increasing concentrations of compound **1** (Figure 3). This quenching of fluorescence was used to perform binding titration experiments. The inset of Figure 3 shows the titration curve for the association of compound **1** to tubulin. Since it was difficult to accurately determine the binding stoichiometry (n) of this ligand, it was set to 1 and the apparent affinity constant was calculated $K_a = (3.75 \pm 1.23) \times 10^5$ M^{-1}. Similar experiments and assumptions were used to determine the binding affinity of the other two analogues. K_a values of $(6.72 \pm 0.88) \times 10^4$ and $(4.01 \pm$

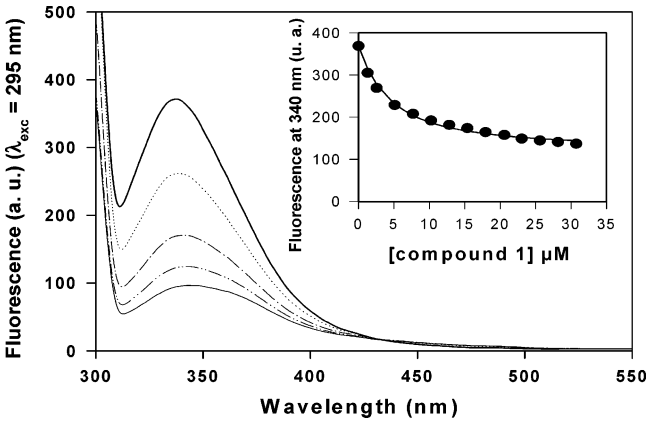

FIGURE 3: Fluorescence changes in the protein emission spectra produced by the binding of compound **1** (excitation at 295 nm): tubulin 2 μM in PG buffer, pH 7(−); tubulin at same concentration with 2.6 μM (···), 10.2 μM (−·−), 20.5 μM (−··−), 30.7 μM (−) of compound **1**. The inset shows the protein fluorescence quenching titration produced by compound **1** binding to 2 μM of tubulin at 25 °C (emission wavelength was 340 nm). Symbol shows experimental data, and line shows the fitted curve (see Materials and Methods) which gives, with a stoichiometry fixed to one, an affinity constant value $K_a = (3.00 \pm 0.11) \times 10^5$ M^{-1} at 25 °C.

1.05) $\times$ 10^4 M^{-1} were found for **2** and **3**, respectively. All the values are the means of three independent determinations. In contrast to compounds **1**−**3**, combretastatin A-4 has an intrinsic fluorescence emission with a maximum at 400 nm (inset of Figure 4A, line b) which interferes with the tryptophanyl emission spectrum of tubulin (inset of Figure 4A, line a). To determine the apparent affinity constant, we first calculated the theoretical emission fluorescence spectra obtained if no binding occurred as a linear combination of the tubulin spectrum (inset of Figure 4A, line a) and combretastatin A-4 (inset of Figure 4A, line b) at a given concentration (inset of Figure 4A, line c) (for more details see Materials and Methods). The calculated spectrum was then subtracted from the one measured in the presence of the complex (inset of Figure 4A, line d). This subtraction was done for each concentration of ligand (Figure 4B). To obtain the titration curve, the values of the differential fluorescence change (ΔF) at 356 nm were plotted as a function of the ligand concentration (inset of Figure 4B) and the data were treated with the method described above for compounds **1**−**3**. The mean of three independent determinations gave an association constant $K_a = (3.35 \pm 1.46) \times 10^6$ M^{-1} for the binding of combretastatin A-4 to tubulin.

2. Isothermal Titration Calorimetry (ITC). Before measuring the interaction by calorimetry, it was important to ensure that there was no tubulin self-association in the presence of the compounds. Analytical ultracentrifugation is very sensitive to the self-association of macromolecules. We examined the association state of tubulin in the presence of the most effective drugs (combretastatin A-4 and compound **1**) by sedimentation velocity measurements. The sedimentation velocity experiment of 0.25 mg/mL tubulin in PG buffer showed a single boundary corresponding to a single sedimenting species. Sedimentation analysis, using a noninteracting species model, led to a value of 5.47 S [5.38; 5.64 S]. With an excess of ligand, similar analyses were performed and sedimentation coefficients of 5.51 S [5.32; 5.85 S] and 5.57 S [5.42; 5.73 S] were found in the presence of combretastatin A-4 and compound **1**, respectively. These

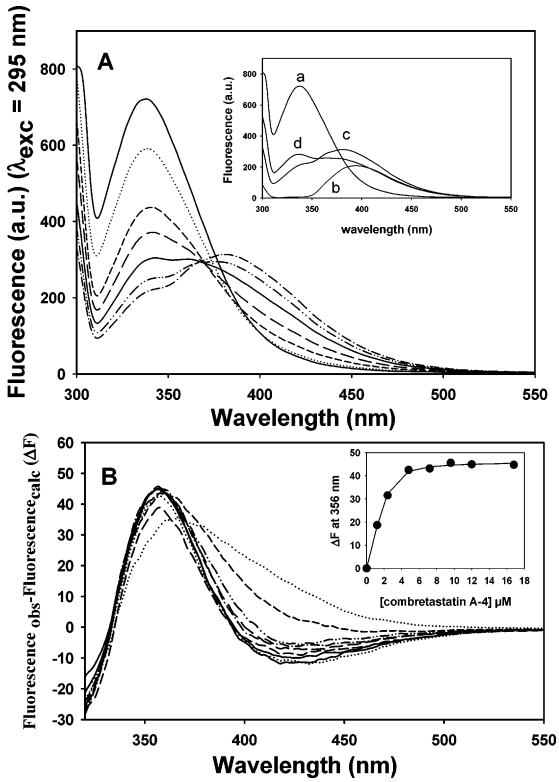

FIGURE 4: Fluorescence changes in the protein emission spectra produced by the binding of combretastatin A-4 (excitation at 295 nm) at 25 °C. (A) Tubulin 2.6 μM in PG buffer, pH 7(−); tubulin at same concentration with 1.2 μM (···), 4.8 μM (- -), 9.6 μM (− −), 16.8 μM (−), 24 μM (−··−), and 28.8 μM (−·−) of combretastatin A-4. The inset shows the experimental emission fluorescence spectra of 2.6 μM of tubulin (a), 28.8 μM of combretastatin A-4 (b), and the complex at same concentration (d). (c) Represents the calculated spectrum of the linear combination of the tubulin and combretastatin A-4 spectra at the same concentration obtained if there was no interaction. (B) Differential fluorescence spectra (ΔF) of tubulin 2.6 μM with 1.2 μM (···), 2.4 μM (- -), 4.8 μM (− −), 7.2 μM (−−), 9.6 μM (−··−), 12 μM (−·−), 14.4 μM (−), and 16.8 μM (···) of combretastatin A-4. The inset shows the differential fluorescence titration curve obtained for the binding of combretastatin A-4 with 2.6 μM of tubulin. Data analyzed as described in Materials and Methods give an affinity constant of (4.08 $\pm$ 0.61) $\times$ 10^6 M^{-1}.

results ruled out the presence of a self-association of tubulin induced by the binding of combretastatin A-4 and its analogues, indicating that isothermal titration calorimetry can be used to determine their binding parameters. A typical isotherm of the combretastatin A-4−tubulin interaction is presented in Figure 5. For this interaction, we calculated an association constant $K_a = (1.88 \pm 0.23) \times 10^6$ M^{-1}, and a number of site of 1.0 $\pm$ 0.1. The interaction was associated with an exothermic heat exchange that allowed a precise enthalpy change determination: $\Delta H = -37.2 \pm 3.3$ kJ mol^{-1}. The resulting binding entropy change was slightly negative, thus, unfavorable to the formation of the complex: $T\Delta S = -1.7 \pm 3.3$ kJ mol^{-1}. The binding of combretastatin A-4 to tubulin is an enthalpy-driven process. Compounds **1**−**3** did not show measurable heat exchanges when they interacted with tubulin. Despite this lack of signal, we were able to measure their affinity constants for tubulin using a displacement ITC method (*12*). Similar affinity constants, as previously measured by fluorescence technique (Table 1), were obtained for combretastatin A-4 and com-

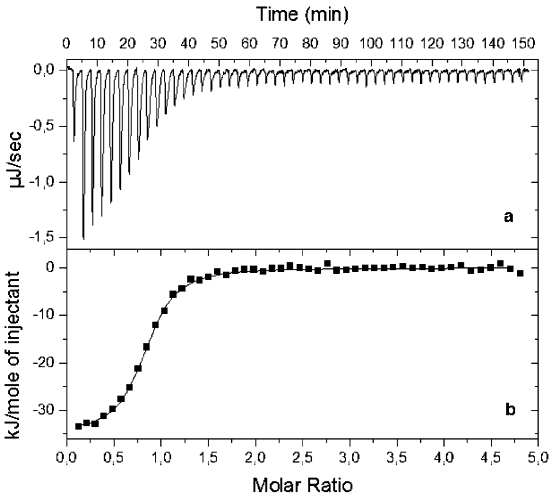

FIGURE 5: Typical ITC profile of the binding of combretastatin A-4 to tubulin in PG buffer at 25°C. (a) Heat signal for the titration after subtraction of the heat of dilution of combretastatin A-4. Tubulin (15 μM) was titrated with 5 μL aliquots of combretastatin A-4 (360 μM). (b) Binding isotherm derived from panel a.

pounds **1** and **2**. For compound **3**, we obtained, by ITC, a 10-fold lower affinity constant than the one obtained by fluorescence. Considering that compound **3** is inactive on in vitro microtubule formation even at a concentration higher than 100 μM, the more reliable affinity constant seems to be the one found by ITC. Moreover, in the fluorescence binding titration assay, tubulin concentration is in the micromolar range, which is too low to determine accurately an affinity constant of 10^3 M^{-1}. To determine such a low affinity constant, we would have to use at least a 10-fold higher tubulin concentration (as in the ITC experiment), but this concentration is incompatible with the technical requirements of fluorescence methods (inner filter effect). The binding entropy change of combretastatin A-4 and compounds **1**−**3** was then calculated (Table 1). In contrast to combretastatin A-4, the binding of compounds **1**−**3** to tubulin is entropy-driven: ΔH was not detectable and the binding entropy change was positive, thus, favorable to the interaction. Indeed, $T\Delta S$ was equal to 28.9 ± 0.4, 24.3 ± 0.8, and 19.7 ± 2.9 kJ mol^{-1} for compounds **1**, **2**, and **3**, respectively.

In conclusion, the chemical modifications of combretastatin A-4 led to compounds presenting a weaker affinity for tubulin. Our thermodynamic results demonstrate that these changes have an enthalpic cost which is not entirely compensated by the rise in entropy.

DISCUSSION

In the previous study (*6*), a series of compounds were synthesized to study their cytotoxicity on human leukemia cell line. Among these molecules, only compounds **1** (IC_{50} = 0.083 μM) and **2** (IC_{50} = 0.52 μM) exhibited a potent cytotoxic activity, through induction of both apoptotic and nonapoptotic signaling pathways. Although first thought to inhibit human topoisomerase I and II, they exhibited a strong antimicrotubule activity. Indeed, these compounds induced a massive accumulation of CEM cells in the G_2/M phase and inhibited purified tubulin polymerization in vitro (*6*). In this report we have shown that, like combretastatin A-4, compounds **1** and **2** exhibit cytotoxic effects (IC_{50} = 0.087 and 0.41 μM, respectively) on the HBL100 cells and lead to a mitotic blockage. This modification in the cell cycle progression was the consequence of an early depolymerization of the microtubule network. In sharp contrast, compound **3** had no effect in both cases. Determination of the thermodynamic parameters by fluorescence and microcalorimetry showed that the most cytotoxic and tubulin polymerization-inhibiting compound, combretastatin A-4, binds tubulin with the highest affinity and that the inactive one binds with the lowest affinity. Moreover combretastatin A-4 binding is enthalpy-driven, whereas the binding of compounds **1**−**3** is entropy-driven. This thermodynamic study shows unambiguously that, to be a good combretastatin analogue, a compound should bind to tubulin with an affinity constant of at least 10^6 M^{-1}, and with an exothermic enthalpy variation. The decrease in affinity for tubulin and the loss of favorable enthalpy variation are correlated with decrease in the ability to inhibit purified tubulin polymerization in vitro, and to modify the microtubule network and the cell cycle of HBL100 cells.

Because colchicine was the first microtubule-destabilizing agent to be discovered, extensive experimental work has been done to localize its binding site. All the experimental data converged to its localization on the β-tubulin subunit at the interface with α-tubulin (*15*), resulting in an inhibition of tubulin polymerization. This binding site has been recently confirmed by determination of the three-dimensional structure of the tubulin−colchicine−stathmin-like domain ternary complex with a resolution of 3.5 Å (PDB code 1SA0) (*7*). A structural analogue of colchicine, DAMA-colchicine, was used to define unambiguously the colchicine orientation in its asymmetric electron density. Because combretastatin A-4 competitively inhibits colchicine binding (*4*), we used these crystallographic data to construct a binding model of the combretastatin analogues−tubulin complex to facilitate the comparison of the activity of these molecules with both colchicine and combretastatin A-4. We superimposed the common structural motif of the combretastatin analogues, which is the trimethoxyphenyl ring, to the colchicine−tubulin complex (A ring in Bailly et al. (*6*) see Materials and Methods) (Scheme 1 and Figure 6). Interestingly, compound **1**, which has a dimethoxyphenyl A-ring, is more active than compounds **2** and **3,** that have a trimethoxyphenyl A-ring similarly to combretastatin A-4 and colchicine. Moreover, only compound **1** has a similar orientation of the 7-methoxy group as combretastatin A-4 and colchicine (Figure 6A). Thus, this orientation seems to be crucial for the activity of such molecules, since compound **1** is more active than compound **2**. Compound **1** presents the methoxy group in front of the β-tubulin Cys 241 (C_β241) which has largely been described to be involved in the interaction of colchicine-site molecules (*15*, *16*).

Recently, Kong et al. developed a model of several boronic combretastatin analogues in which there is a strong hydrogen bonding between the boronic acid moiety and both Thr179 and Val181 of α-tubulin (*17*). Using structurally different molecules, we confirmed the importance of these two residues in the colchicine derivatives binding to tubulin. When we observed the C-ring at the opposite site of the molecules, compounds **1**, **2**, and combretastatin A-4 have a hydroxyl group in 3′ position and differ from colchicine which has a carbonyl group at the same position. These functional groups are hydrogen bond donor or acceptor and

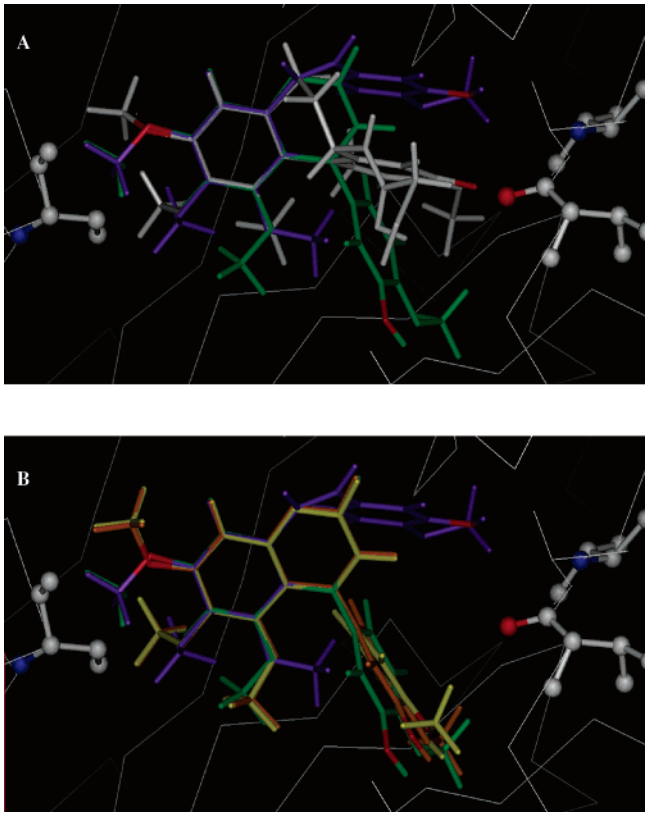

FIGURE 6: Model of combretastatin A-4 and analogues binding in the colchicine site of tubulin. (A) Superimposition of the trimethoxyphenyl ring A of combretastatin A-4 (violet), compound **1** (green) to colchicine (white) in the tubulin binding site. (B) Superimposition of compounds **1** (green), **2** (orange), and **3** (yellow) to combretastatin A-4 (violet). The important amino acids for specific hydrogen bonds are represented in white ball-and-stick. Compounds are in Stick representation. Atoms which are hydrogen bond donor or acceptor for the compounds−tubulin complex are in red (oxygen) and in blue (nitrogen). Colchicine could form a hydrogen bond with Val181. Compounds **1**, **2**, and combretastatin A-4 could form a hydrogen bond with Thr179 of α-tubulin.

differ in the distance of two amino acids of α-tubulin, Thr179 and Val181. The carbonyl group in colchicine could form a hydrogen bond with the amide group of Val181 peptide chain. The hydroxyl group of compounds **1**, **2**, and combretastatin A-4 could form a hydrogen bond with the carboxyl group of Thr179 peptide chain. For molecules having a hydroxyl group in the 3′ position, hydrogen bond formation between this group and the Thr179 of α-tubulin is thermodynamically easier in the case of combretastatin A-4 than in the case of compounds **1** and **2** because of a greater proximity. This observation explained first the decrease in binding affinity, as hydrogen bond is generally synonym of binding specificity. Second, it was also in agreement with the different thermodynamic behavior found by microcalorimetry between the combretastatin A-4 and its analogues. Indeed, only the binding of combretastatin A-4 was associated with an exothermic heat exchange that allowed a precise enthalpy change determination traducing hydrogen bond formation in the complex.

Recently, an important molecular modeling (*16*) study, realized on a large panel of known colchicine site inhibitors, suggested the important role of hydrogen bond formation between the colchicine site inhibitor and the Thr179 of α-tubulin. The authors concluded that an ideal colchicine site inhibitor should have three hydrogen bond acceptors, one hydrogen bond donor, two hydrophobic centers, and one planar group (*16*). Our molecular modeling confirmed the important role of this amino acid and demonstrated that the decrease in hydrogen bond formation leads to a decrease in affinity for tubulin and in antitubulin cellular biological activity. Like the large set of colchicine site inhibitors studied by Nguyen et al. (*16*), our molecules have the structural criteria needed for a colchicine site inhibitor.

In summary, we have found that the biological activity of our compounds previously synthesized as potential topoisomerase inhibitors is correlated to their molecular binding to tubulin in vitro. The presence of these molecules in the cytosol leads to an accumulation of the HBL100 cells in G_2M phase. We have demonstrated that this modification is a consequence of a depolymerization of the microtubule network that was already shown using purified tubulin in vitro (*6*). We showed that, although combretastatin A-4 remains the most active compound, compounds **1** and **2** have a rather good antitubulin activity and that the greater the affinity of the compound for tubulin is, the more biologically active it is. Superimposition of the combretastatin A-4 and these analogues in the tubulin colchicine site indicated that the orientation of the methoxy group in 7 position of the ring A of **1** is responsible for the biological activity of this type of molecule. Further work is thus required to synthesize other molecules that keep this important orientation in ring A but increase the hydrogen bond formation of the ring C with Thr179 of α-tubulin.

Finding new microtubule-damaging agent which can be used for their cytotoxicity in tumor cells has been an important therapeutic strategy. The evidence of angiogenesis dependence of tumor growth(*18*) allowed sudden awareness of the importance of chemical molecules acting as angiogenesis inhibitors to stop the tumor growth, thus, opening a new therapeutic approach. In particular, antitubulin agents seem to be the most potent antiangiogenic agents (*19*−*20*), but the mechanism by which tubulin is implicated has not been clearly elucidated yet. For paclitaxel, increase in microtubule dynamics has been implicated in its antiangiogenic activity (*21*), suggesting a key role of microtubule dynamics in this phenomenon. Since combretastatin A-4 is in clinical trial for its antiangiogenic property, relationships between antiangiogenic activity and microtubules dynamics, for this series of combretastatin analogues, should be further investigated.

ACKNOWLEDGMENT

We are very grateful to Mrs. Soazig Malesinsky and Dr. François Devred for helpful discussions and reading the manuscript, Prof. Didier Siri for the minimization of molecule structure, and “Alazard et Roux” slaughter house (Tarascon, France) for the lamb brain necessary for tubulin purification.

REFERENCES

1. Jordan, M. A., and Wilson, L. (2004) Microtubules as a target for anticancer drugs, *Nat. Rev. Cancer 4*, 253−265.
2. Pettit, G. R., Singh, S. B., Hamel, E., Lin, C. M., Alberts, D. S., and Garcia-Kendall, D. (1989) Isolation and structure of the strong cell growth and tubulin inhibitor combretastatin A-4, *Experientia 45*, 209−211.

3. Tozer, G. M., Kanthou, C., Parkins, C. S., and Hill, S. A. (2002) The biology of the combretastatins as tumour vascular targeting agents, *Int. J. Exp. Pathol. 83*, 21−38.
4. Lin, C. H., Singh, S. B., Chu, P. S., Dempcy, R. O., Schmidt, J. M., Pettit, G. R., and Hamel, E. (1988) Interactions of tubulin with potent natural and synthetic analogs of the antimitotic agent combretastatin: a structure−activity study. *Mol. Pharmacol. 34*, 200−206.
5. Ohsumi, K., Hatanaka, T., Fujita, K., Nakagawa, R., Fukuda, Y., Nihei, Y., Suga, Y., Morinaga, Y., Akiyama Y., and Tsuji,T. (1998) Syntheses and antitumor activity of cis-restricted combretastatins: 5-membered heterocyclic analogs, *Bioorg. Med. Chem. Lett. 8*, 3153−3158.
6. Bailly, C., Bal, C., Barbier, P., Combes, S., Finet, J.-P., Hildebrand, M.-P., Peyrot, V., and Wattez, N. (2003) Synthesis and biological evaluation of 4-arylcoumarin analogues of combretastatins, *J. Med. Chem. 46*, 5437−5444.
7. Ravelli, R. B., Gigant, B., Curmi, P. A., Jourdain, I., Lachkar, S., Sobel, A., and Knossow, M. (2004) Insight into tubulin regulation from a complex with colchicine and a stathmin-like domain, *Nature 428*, 198−202.
8. Weisenberg, R. C., Borisy, G. G., and Taylor, E. W. (1968) The colchicine-binding protein of mammalian brain and its relation to microtubules, *Biochemistry 1*, 4466−4479.
9. Lee, Y. C., Frigon, R. P., and Timasheff, S. N. (1973) The chemical characterization of calf brain microtubule protein subunits, *J. Biol. Chem. 248*, 7253−7262.
10. Andreu, J. M., Gorbunoff, M. J., Lee, J. C., and Timasheff, S. N. (1984) Interaction of tubulin with bifunctional colchicine analogs: an equilibrium study, *Biochemistry 23*, 1742−1752.
11. Lakowicz, J. R. (1983**)** *Principles of Fluorescence Spectroscopy*, Plenum Press, New York.
12. Sigurskjold, B. W., Berland, C. R., and Svensson, B. (1994) Thermodynamics of inhibitor binding to the catalytic site of glucoamylase from *Aspergillus niger* determined by displacement titration calorimetry, *Biochemistry 33*, 10191−10199.
13. Sigurskjold, B. W. (2000) Exact analysis of competition ligand binding by displacement isothermal titration calorimetry, *Anal. Biochem. 277*, 260−266.
14. Schuck, P., and Rossmanith, P. (2000) *Biopolymers 54*, 328−341.
15. Bai, R., Covell, D. G., Pei, X. F., Ewell, J. B., Nguyen, N. Y., Brossi, A., and Hamel, E. (2000) Mapping the binding site of colchicinoids on β-tubulin: 2-chloroacetyl-2-demethylthiocolchicine covalently reacts predominantly with cysteine 239 and secondary with cysteine 354, *J. Biol. Chem. 275*, 40443−40452.
16. Nguyen, T. L., McGrath C., Hermone, A. R., Burnett, J. C., Zaharevitz, D. W., Day, B. W., Wipf, P., Hamel, E., and Gussio, R. (2005) A common pharmacophore for a diverse set of colchicine site inhibitors using a structure-based approach, *J. Med. Chem. 48*, 6107−6116.
17. Kong, Y., Grembecka, J., Edler, M. C., Hamel, E., Mooberry, S. L., Sabat, M., Rieger, J., and Brown, M. L. (2005**)** Structure-based discovery of a boronic acid bioisostere of combretastatin A-4, *Chem. Biol. 12*, 1007−1014.
18. Folkman, J. (1992)The role of angiogenesis in tumor growth, *Semin. Cancer Biol. 3*, 65−71.
19. Baguley, B. C., Holdaway, K. M., Thomsen, L. L., Zhaung, L., and Zwi, L. J. (1991) Inhibition of growth of colon 38 adenocarcinoma by vinblastine and colchicine: evidence for vascular mechanism, *Eur. J. Cancer 27*, 482−487.
20. Belotti, D., Vergani, V., Drudis, T., Borsotti, P., Pitelli, M. R., Giavazzi, R., and Taraboletti, G. (1996) The microtubule-affecting drug paclitaxel has an antiangiogenic activity, *Clin. Cancer Res. 2*, 1843−1849.
21. Pasquier, E., Honoré S., Pourroy, B. Jordan, M. A., Lehmann, M., Briand, C., and Braguer, D. (2005) Antiangionenic concentrations of paclitaxel induce an increase in microtubule dynamics in endothelial cells but not in cancer cells, *Cancer Res. 65*, 2433−2440.

BI060476G